AFRL-RZ-WP-TP-2012-0146

ELECTROMAGNETIC CHARACTERIZATION OF $YBa_2Cu_3O_{7-\delta}$ THIN FILMS WITH CALCIUM DOPING FOR BI-CRYSTAL GRAIN BOUNDARY CONDUCTIVITY ENHANCEMENT (POSTPRINT)

Richard A. Kleismit and Gregory Kozlowski

Wright State University

Angela L. Campbell, Timothy J. Haugan, Rand R. Biggers, Paul N. Barnes, and Timothy L. Peterson

Mechanical Energy Conversion Branch
Energy/Power/Thermal Division

Iman Maartense

University of Dayton Research Institute

Simon C. Hopkins

University of Cambridge

FEBRUARY 2012

AIR FORCE RESEARCH LABORATORY
PROPULSION DIRECTORATE
WRIGHT-PATTERSON AIR FORCE BASE, OH 45433-7251
AIR FORCE MATERIEL COMMAND
UNITED STATES AIR FORCE

REPORT DOCUMENTATION PAGE

Form Approved
OMB No. 0704-0188

1. REPORT DATE *(DD-MM-YY)*	2. REPORT TYPE	3. DATES COVERED *(From - To)*
February 2012	Journal Article Postprint	24 January 2006 – 24 January 2008

4. TITLE AND SUBTITLE

ELECTROMAGNETIC CHARACTERIZATION OF $YBa_2Cu_3O_{7-\delta}$ THIN FILMS WITH CALCIUM DOPING FOR BI-CRYSTAL GRAIN BOUNDARY CONDUCTIVITY ENHANCEMENT (POSTPRINT)

5a. CONTRACT NUMBER
In-house

5b. GRANT NUMBER

5c. PROGRAM ELEMENT NUMBER
62203F

6. AUTHOR(S)

Richard A. Kleismit and Gregory Kozlowski (Wright State University)
Angela L. Campbell, Timothy J. Haugan, Rand R. Biggers, Paul N. Barnes, and Timothy L Peterson (AFRL/RZPG)
Iman Maartense (University of Dayton Research Institute)
Simon C. Hopkins (University of Cambridge)

5d. PROJECT NUMBER
3145

5e. TASK NUMBER
32

5f. WORK UNIT NUMBER
314532ZE

7. PERFORMING ORGANIZATION NAME(S) AND ADDRESS(ES)

Wright State University
Physics Department
Dayton, OH 45435

Mechanical Energy Conversion Branch (AFRL/RZPG)
Energy/Power/Thermal Division
Air Force Research Laboratory, Propulsion Directorate
Wright-Patterson Air Force Base, OH 45433-7251
Air Force Materiel Command, United States Air Force

University of Dayton Research Institute
Dayton, OH 45469

University of Cambridge
Department of Materials Science and Metallurgy
Pembroke Street
Cambridge, CB2 3QZ, UK

8. PERFORMING ORGANIZATION REPORT NUMBER
AFRL-RZ-WP-TP-2012-0146

9. SPONSORING/MONITORING AGENCY NAME(S) AND ADDRESS(ES)

Air Force Research Laboratory
Propulsion Directorate
Wright-Patterson Air Force Base, OH 45433-7251
Air Force Materiel Command
United States Air Force

10. SPONSORING/MONITORING AGENCY ACRONYM(S)
AFRL/RZPG

11. SPONSORING/MONITORING AGENCY REPORT NUMBER(S)
AFRL-RZ-WP-TP-2012-0146

12. DISTRIBUTION/AVAILABILITY STATEMENT

Approved for public release; distribution unlimited.

13. SUPPLEMENTARY NOTES

Journal article published in *Superconductor Science and Technology*, Vol. 21, 2008. This paper contains color.

 Work on this effort was completed in 2008. PA Case Number: 88ABW-2008-0150; Clearance Date: 24 January 2008.

14. ABSTRACT

The objective of this study was to examine the transport properties of two $YBa_2Cu_3O_{7-\delta}$ thin films with $(Y_{0.9}Ca_{0.1})_2BaCuO_5$ additions deposited on vicinal $SrTiO_3$ 6° bi-crystal substrates and to investigate the possible correlations between spatial calcium distribution and local electromagnetic properties across bi-crystal grain boundaries using evanescent microwave microscopy (EMM) and atomic force microscopy (AFM). The samples under consideration differed in transport critical current measurements by a factor of two although they were deposited on the same type of bi-crystal substrate. A near-field evanescent microwave microscope based on a coaxial transmission line resonator with an end-wall aperture was used to measure changes in conductivity local to the bi-crystal boundary of $YBa_2Cu_3O_{7-\delta}$ thin films below (79.2 K) and above (room temperature) the superconducting transition temperature. Atomic concentration measurements by electron microprobe analysis were performed in the same regions, and a clear correlation between calcium distribution and conductivity at 79.2 K (as represented by the change in quality factor) was found. Surface potential imaging (SPI) and quality factor scans in the area of the bi-crystal grain boundaries were performed at room temperature using AFM and EMM, respectively, to evaluate local electromagnetic properties in the normal state and investigate their correlation with superconducting properties.

15. SUBJECT TERMS

transport, microprobe, analysis, atomic, measurements, samples, grain, boundaries, evanescent, microwave

16. SECURITY CLASSIFICATION OF:			17. LIMITATION OF ABSTRACT:	18. NUMBER OF PAGES	19a. NAME OF RESPONSIBLE PERSON (Monitor)
a. REPORT	b. ABSTRACT	c. THIS PAGE			Timothy J. Haugan
Unclassified	Unclassified	Unclassified	SAR	12	19b. TELEPHONE NUMBER *(Include Area Code)* N/A

Supercond. Sci. Technol. **21** (2008) 035008 (6pp) doi:10.1088/0953-2048/21/3/035008

Electromagnetic characterization of $YBa_2Cu_3O_{7-\delta}$ thin films with calcium doping for bi-crystal grain boundary conductivity enhancement

Richard A Kleismit[1], Angela L Campbell[2], Gregory Kozlowski[1,3], Timothy J Haugan[2], Rand R Biggers[2], Iman Maartense[2], Simon C Hopkins[3], Paul L Barnes[2] and Timothy L Peterson[2]

[1] Physics Department, Wright State University, Dayton, OH 45435, USA
[2] Materials and Manufacturing Directorate, Air Force Research Laboratory, Wright-Patterson AFB, OH 45433, USA
[3] Department of Materials Science and Metallurgy, University of Cambridge, Pembroke Street, Cambridge CB2 3QZ, UK

E-mail: gregory.kozlowski@wright.edu and gk286@cam.ac.uk

Received 8 November 2007, in final form 19 December 2007
Published 8 February 2008
Online at stacks.iop.org/SUST/21/035008

Abstract

The objective of this study was to examine the transport properties of two $YBa_2Cu_3O_{7-\delta}$ thin films with $(Y_{0.9}Ca_{0.1})_2BaCuO_5$ additions deposited on vicinal $SrTiO_3$ 6° bi-crystal substrates and to investigate the possible correlations between spatial calcium distribution and local electromagnetic properties across bi-crystal grain boundaries using evanescent microwave microscopy (EMM) and atomic force microscopy (AFM). The samples under consideration differed in transport critical current measurements by a factor of two although they were deposited on the same type of bi-crystal substrate. A near-field evanescent microwave microscope based on a coaxial transmission line resonator with an end-wall aperture was used to measure changes in conductivity local to the bi-crystal boundary of $YBa_2Cu_3O_{7-\delta}$ thin films below (79.2 K) and above (room temperature) the superconducting transition temperature. Atomic concentration measurements by electron microprobe analysis were performed in the same regions, and a clear correlation between calcium distribution and conductivity at 79.2 K (as represented by the change in quality factor) was found. Surface potential imaging (SPI) and quality factor scans in the area of the bi-crystal grain boundaries were performed at room temperature using AFM and EMM, respectively, to evaluate local electromagnetic properties in the normal state and investigate their correlation with superconducting properties.

(Some figures in this article are in colour only in the electronic version)

1. Introduction

Grain boundaries in polycrystalline $YBa_2Cu_3O_{7-\delta}$ (YBCO) superconducting thin films represent major obstacles for the transport current and quite significantly restrict their broader commercialization. The critical current density is initially constant within a few degrees of misalignment, but then decreases exponentially as a function of the misorientation angle between adjacent grains [1–3]. The critical current density of grain boundaries can be increased in YBCO by partial substitution of calcium for yttrium. Calcium put preferentially into grain boundaries reduces hole (superconducting carrier) depletion and results in up to a 35% increase in the critical current density for a 20° boundary misalignment [4]. The charge redistribution, which exists in grain boundaries or at interfaces, results from a very large dielectric constant that increases exponentially with temperature above 160 K [5] and low carrier densities in high

temperature superconductors. This redistribution creates a spatially extended and a positively charged region (depletion zone) and causes the energy bands to bend down on the scale of the coherence length [6]. From theoretical calculations done by Schwingenschlögl *et al* [7] it appears that up to 0.1 holes on average are depleted per intraplane Cu site for high temperature superconductors in the normal state. Additionally, strain, which sometimes exceeds 10% at dislocation cores in the grain boundary area [6], is another reason to have an excess of oxygen vacancies (or hole depletion) at boundaries.

The positive role of preferential calcium doping of grain boundaries to enhance the critical current density in high temperature superconductors is most commonly understood to occur by the replacement of trivalent yttrium by divalent calcium of the same size to create an extra hole in the grain boundary area. However, the presence of compressive or tensile strain regions at the boundary provides another energetically favorable alternative: the replacement of barium or copper with calcium, which relieves the strain and in turn suppresses oxygen vacancies [6]. In addition, according to Schmehl *et al* [8], local hole doping via Ca additions up to 0.3 holes/CuO_2 unit results in a significant reduction of energy band bending at the grain boundary, and consequently the grain boundary charge and the space charge region are also reduced. In summary, we can say that preferential calcium additions have a beneficial effect in reduction of the charge redistribution and minimization of charge and strain fields at grain boundaries. Above all, addition of calcium creates extra holes (carriers) or reduces depletion of holes in the boundaries and leads to an improvement in the current carrying capability. Mohan *et al* [9] have also found that the normal state resistivity of YBCO thin films decreases with increased Ca doping, with a simultaneous decrease in the critical temperature.

By better understanding bi-crystal grain boundary behavior, we can engineer grain boundaries with improved properties. This is a major challenge in superconductor research and is essential for the commercialization of high temperature superconducting wire. It has been shown that evanescent microwave microscopy (EMM) and surface potential imaging (SPI) through the use of atomic force microscopy (AFM) are well suited for the non-destructive evaluation of surface and subsurface properties of materials, including flaw and failure detection in manufacturing applications. The unique features of the evanescent microwave probe allow one to perform quantitative measurements of different material properties, such as complex permittivity, below the surface as well as at the surface because of its penetration depth. SPI maps of the electrostatic potential on the sample surface will change due to local variation in electromagnetic properties and thus provide data complementary to the EMM data.

The objective of this study is to utilize an evanescent microwave probe and SPI in the characterization of YBCO thin films with $(Y_{0.9}Ca_{0.1})_2BaCuO_5$ additions deposited on vicinal $SrTiO_3$ bi-crystal substrates with a 6° misorientation angle. The investigation provides a correlation between evanescent microscopy and microprobe elemental analysis data, deposition parameters, and transport current measurements. In addition, surface potential imaging is used to check for macroscopic charge redistribution at the bi-crystal grain boundaries in YBCO thin films at room temperature when real and imaginary parts of permittivity due to dipolar polarization associated with the hopping motion of localized charge carriers are extremely large [5]. As a result of this charge redistribution, the energy bands will bend down and establish a positive charge (depletion zone), especially, in the bi-crystal grain boundary area which will be diminished by Ca doping [6]. This is opposite to the conclusion by Su and Welch [10] based on the theoretical considerations and to holography data by Schofield *et al* [11] which conclude that the energy bands bend up. Such bending would cause the grain boundary plane to be negative for undoped YBCO, and Ca doping would further increase the negative charge there causing the energy bands to bend up even more. Kalinin *et al* [12], who studied a $SrTiO_3$ bi-crystal grain boundary using a surface potential imaging technique, have concluded that the width of the depletion zone at the boundary area depends not only on tip-bias induced band bending but also on capacitive interaction between the tip and the surface of the material under consideration, its volume and surface bound charges, double layers and remanent polarization.

2. Experimental procedure

YBCO and multilayer $\{M_x/(YBCO)_y\}\cdot N$ films, where $M = (Y_{0.9}Ca_{0.1})_2BaCuO_5 = (Y, Ca)211$, x and y are layer thicknesses and N is the number of layers, were deposited by pulsed laser deposition as described previously [13, 14]. Deposition parameters were 248 nm laser wavelength, ~3.2 J cm^{-2} laser fluence, 25 nm pulse length, 2–4 Hz laser repetition rate, 5.5 cm target-to-substrate distance, 90–92% dense targets, 300 mTorr oxygen partial pressure, and a post-deposition anneal at 500 °C in one atmosphere of oxygen [14]. The heater block temperature was 775–800 °C. The substrates were (010) c-axis tilted $SrTiO_3$ with one side epi-polished, and total grain boundary misorientation of 6° [1]. For multilayer films, an automated target rotation and pulse-triggering system was used to control the deposition sequences, with a period of about 13 s during which the deposition was stopped and different targets were rotated into position. For this study, the (Y, Ca)211 particles deposited by island growth, however also with an ultrathin layer ~0.1–0.2 nm of Y–Ca–Ba–Cu–O with exact composition unknown [15]. Both the nanoparticles and ultrathin layer could be observed with TEM cross-sections [15].

The deposition rates of both (Y, Ca)211 and YBCO (calibrated before deposition) were used with the deposition times to estimate the thickness of both layers. Deposition rates for YBCO and (Y, Ca)211 were 9–12 nm min^{-1} and 14–18 nm min^{-1}, respectively (1.55 times higher for (Y, Ca)211 than for YBCO). The total film thickness was kept in the range of 0.15–0.25 μm to provide consistent comparisons. Every sample was measured multiple times across acid-etched step edges with a profilometer (KLA-Tencor, P15) to obtain the film thickness with an error <5%.

Two multilayer films were selected for the detailed characterization of Ca-doped samples reported here. Sample A

Table 1. Sample parameters.

Deposition temperature (°C)	Roughness RMS value (nm) inside/outside boundary	T_C (K)	Surface potential change (mV) at room temperature	Quality factor change (10^5) at room temperature	Transport current density J_C (MA cm^{-2})
775 (sample A)	22.4/13.3	88.9	33	0.29	1.8
800 (sample B)	13.6/13.1	89.4	14	0.88	3.9

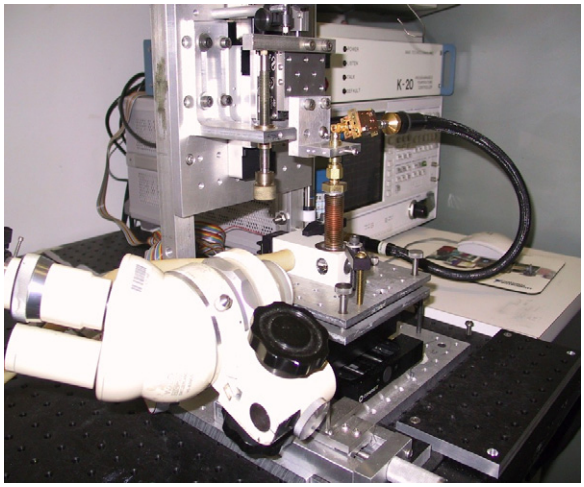

Figure 1. Evanescent microwave microscopy system.

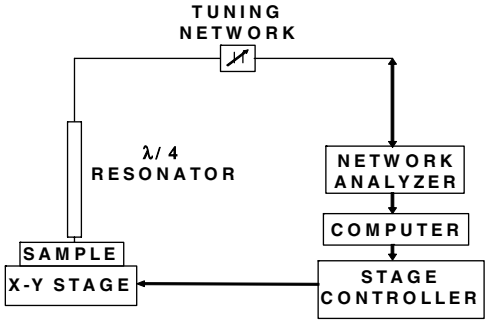

Figure 2. Evanescent microwave microscopy arrangement for measuring local permittivity.

was 0.12 μm thick, with structure {M$_{\sim 0.4\ nm}$/YBCO$_{\sim 7\ nm}$}·16, and was deposited with a substrate temperature of 775 °C. Sample B was deposited on a substrate at 800 °C, with structure {M$_{\sim 0.4\ nm}$/YBCO$_{\sim 7\ nm}$}·21 and total thickness 0.16 μm. The nominal volume fraction of (Y, Ca)211 phase was ∼5.7%, and overall Ca concentration was 0.18% by molar fraction, in both samples. Relevant properties of samples A and B are given in table 1.

The evanescent microwave microscopy system shown in figures 1 and 2 was adapted for making cryogenic measurements by attaching a miniature single-stage Joule–Thompson cryogenic system to the X–Y stage. The microwave probe was fitted through a bellows providing a vacuum seal and allowing the probe to move freely over the sample, which was mounted on the cryogenic finger directly below the probe tip [16]. The microscope probe consists of a tuned, end-wall apertured coaxial transmission line. The resonator probe is coupled to the network analyzer through the tuning network and coupled to the sample. When the resonator tip is in close proximity to the sample, the resonator's frequency f_0 will shift along with corresponding changes ΔQ in the quiescent quality factor Q_0 of the resonator [16, 17].

Surface potential imaging is a nulling technique. The atomic force microscope (Veeco multimode scanning probe microscope with a nanoscope IIIa controller and Quadrex phase detection) mapped the electrostatic potential on the sample surface with 0.5 V applied to the samples. When the tip was traveling above the sample surface in LiftMode, the tip experienced a force whenever the potential on the surface was different from the tip potential. The voltage applied to the tip to nullify the force was plotted versus the in-plane coordinates to create three-dimensional surface potential images [18].

The superconducting transition temperature (T_c) was measured using an AC susceptibility technique with the amplitude of the magnetic sensing field strength varied from 0.025–2.2 Oe, at a frequency of approximately 4 Hz. Note that AC susceptibility provides information about primary and secondary transitions of the entire film, rather than the best continuous superconducting path that is obtained with resistive T_c measurements. Transport J_c measurements were made by a four-point contact method, with microbridges 0.03–0.05 cm wide by 0.3 cm length and an electric field criterion of 1 μV cm^{-1}. Microbridges were made by 248 nm UV laser etching through alumina masks with laser fluence 0.1 J cm^{-2}, laser pulse length 25 ns, and at 1 Hz. The critical current was measured in liquid nitrogen at 77.2 K. Current was applied to the sample by a step-ramp method: a current step interval of 0.2–0.5 s, a ramp rate of 0.25–1.0 A s^{-1}, and a voltage sample period from 2× to 4× smaller than the current step interval were used. The maximum current step size was 0.1 A.

The films were imaged by scanning electron microscopy in ultrahigh resolution mode (SEM, FEI-Sirion). Characterization of the surface topography together with surface potential mapping were both performed using AFM at 298 K, particularly in the region of each bi-crystal boundary. Several maps were acquired with raster series of 25 μm × 25 μm and 50 μm × 50 μm at separate locations along and outside the bi-crystal grain boundary area, and average effective surface potential values were calculated for each region. The evanescent microwave microscopy scans, with a resolution of ∼1 μm and the capability to detect changes in local dielectric properties of the material on the order of ∼10^{-3}, were performed at temperatures of 79.2 and 298 K and measured a change ΔQ in quality factor of the resonator, which is directly related to changes in the local conductivity. The scan parameters for samples A and

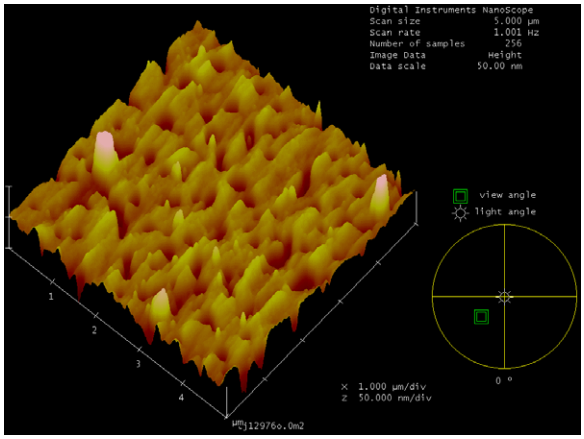

Figure 3. Surface morphology of sample (A) outside the bi-crystal boundary.

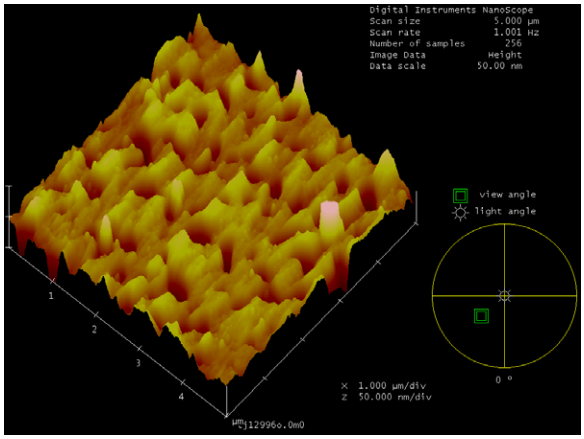

Figure 4. Surface morphology of sample (B) outside the bi-crystal boundary.

B are $f_{0A} = 1.2516$ GHz and $f_{0B} = 1.2373$ GHz with a probe tip standoff distance of 2 μm. Data were taken at 0.07 μm step intervals over a total scan length of 35 μm centered at the bi-crystal boundary. Electron microprobe analysis was performed using the same line scan region during the evanescent probe scans, and Ca intensity values will be presented in this paper for the central 15 μm range spanning the bi-crystal boundary.

3. Results

Despite the similar deposition conditions, samples A and B had significantly different superconducting properties. Sample A had a T_c of 88.9 K and J_c, at 77.2 K in self-field, of 1.8 MA cm^{-2}; the T_c of sample B was slightly higher at 89.4 K, but at 3.9 MA cm^{-2} J_c was more than double that of sample A (table 1).

The three-dimensional surface images obtained by AFM far from the bi-crystal boundaries of the YBCO thin films doped with (Y, Ca)211 additions are shown in figures 3 and 4 for samples A and B, respectively. The average rms roughness for both samples is similar: 13.3 nm for sample A and 13.1 nm

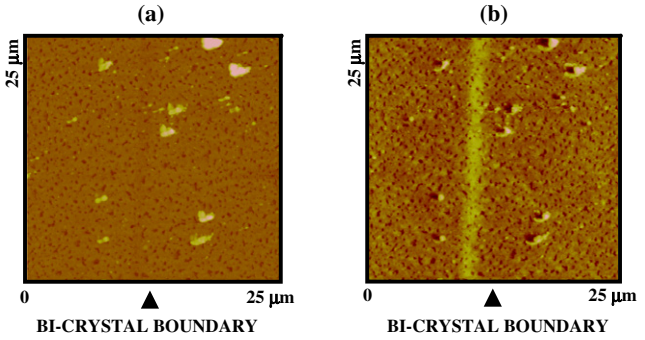

Figure 5. Planar view of roughness (a) and surface potential (b) for sample (A) in the vicinity of the bi-crystal boundary.

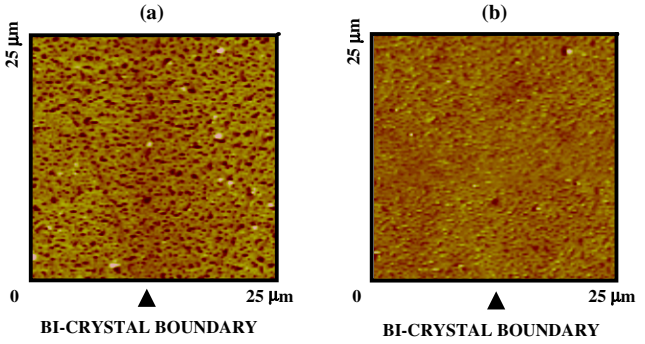

Figure 6. Planar view of roughness (a) and surface potential (b) for sample (B) in the vicinity of the bi-crystal boundary.

for sample B. A planar view of topography together with a surface potential map in the vicinity of the bi-crystal boundary is presented in figure 5 (sample A) and figure 6 (sample B). Whereas the rms values were very similar far away from the boundary, the average rms roughness in the vicinity of the boundary is almost two times higher for sample A than B, with values of 22.4 nm and 13.6 nm respectively. The bi-crystal grain boundary is barely visible in the micrographs, and its location is clearer for sample A (figure 5(a)) than for sample B (figure 6(a)). On the other hand, the surface potential at 298 K has a distinct band of elevated values along the grain boundary for sample A, which had the lower transport current density (see table 1 and figure 5(b)). The stepwise increase of the potential is 35 mV for sample A and only 14 mV for sample B (see table 1). As a result of this smaller increase, the variation of surface potential over the bi-crystal boundary is not visible in the image for sample B (figure 6(b)).

Evanescent microwave microscopy line scans across the bi-crystal boundaries for samples A and B at 79.2 K are presented in figure 7, showing the change in quality factor with position. Figure 8 shows the corresponding variation in calcium intensity, from electron microprobe analysis, along the same lines. The bi-crystal boundary is at approximately 7.5 μm in every case. Because the evanescent probe appeared to be averaging the data due to the wider spread of the evanescent field emanating from the tip, the microprobe scan data in figure 8 are presented after the application of a 20-point moving average smoothing algorithm to aid comparison

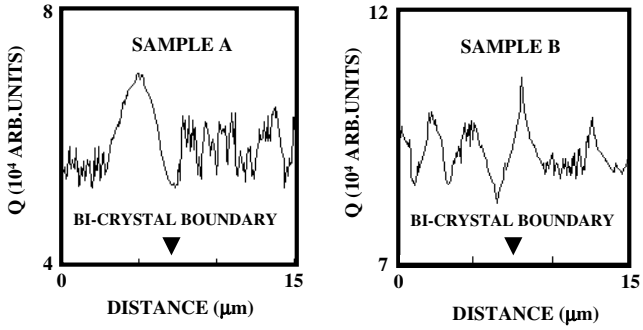

Figure 7. Evanescent microwave change in Q scan image for YBCO thin film at 79.2 K for sample (A) and (B).

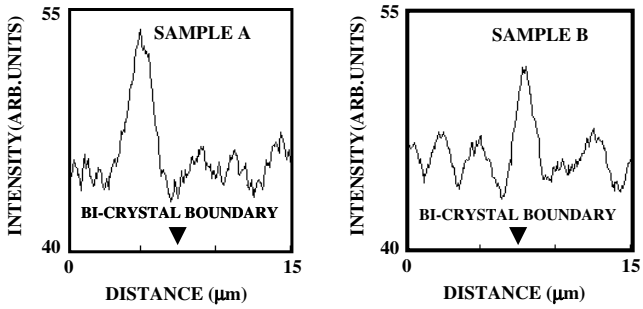

Figure 8. Microprobe line scan of elemental calcium content across the bi-crystal boundary at room temperature for sample (A) and (B).

with the evanescent ΔQ scans. The agreement between peak positions and relative intensities for the evanescent microwave scans in figure 7 and the electron microprobe scans in figure 8 is excellent, demonstrating that surface conductivity (in the superconducting state) is extremely well correlated with local calcium concentration.

The mean x-ray intensity levels for calcium in sample A are much lower than those of sample B exactly at the bi-crystal junction (see figure 7). Remember that the same amount of calcium was added to both films, but the films were deposited at different temperatures: sample A at 775 °C and sample B at 800 °C. In figures 7 and 8, the largest peak (for both calcium content and ΔQ) is closer to the bi-crystal grain boundary for sample B than sample A. This suggests a much better conductivity across the boundary for sample B.

Figure 9 represents two-dimensional ΔQ scans taken at room temperature ($T = 298$ K) and suggests a significant overall increase in the normal state conductivity of sample B with respect to sample A (see table 1). The average quality factor change ΔQ increases by a factor of three from 0.29×10^5 (sample A) to 0.88×10^5 (sample B).

4. Summary

The clear correlation between the change of quality factor from evanescent microscopy scans and the local calcium content from electron microprobe analysis demonstrates that calcium is responsible for increased local conductivity, perhaps due to an enhancement of local charge carrier concentration. The same correlation was not found for yttrium, barium or copper concentrations (not presented here), suggesting that the effect was associated with calcium and not directly with impurity phases or thickness. Sample porosity and thickness variations, however, preclude the quantitative determination of conductivity and calcium concentration in these samples.

Sample B had a critical current density more than double that of sample A, despite the same average calcium concentration and qualitatively similar spatial variations of calcium content and conductivity (figures 7 and 8). Sample B had a higher average value of ΔQ, both at room temperature (0.88×10^5 compared to 0.29×10^5) and in the superconducting state, than sample A, suggesting globally higher conductivity; and in addition, at 79.2 K, sample B showed a maximum in ΔQ at the bi-crystal boundary in contrast to sample A's minimum, which would suggest improved grain boundary transport properties.

A higher deposition temperature was used for sample B (800 °C) than sample A (775 °C), which may have been responsible for the improved conductivity and critical current performance, perhaps by enhancing calcium transport into the grain boundaries. Indeed, the critical temperature is slightly higher in sample B than sample A (89.4 K compared to 88.9 K), which would be consistent with lower intragrain

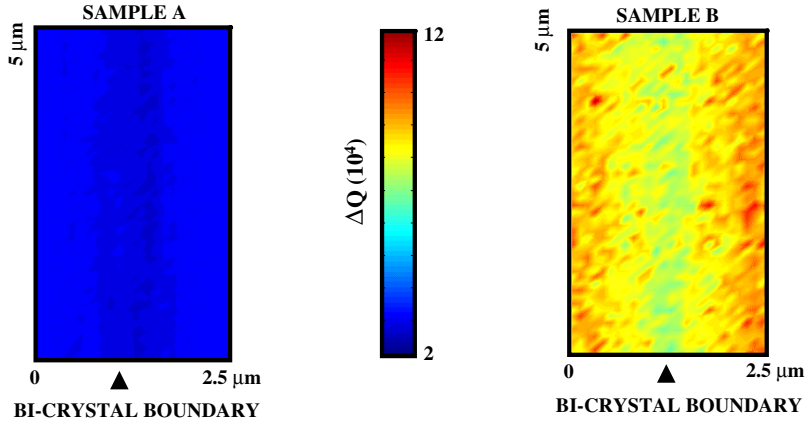

Figure 9. Evanescent microwave change in Q scan image for YBCO thin film at room temperature for sample (A) and (B).

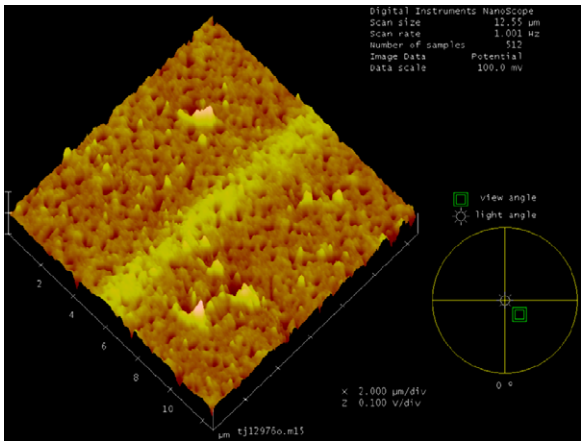

Figure 10. Three-dimensional view of surface potential for sample (A) in the vicinity of the bi-crystal boundary.

calcium concentrations. (There are considerable experimental data to show that calcium doping in grains causes a substantial decrease in the critical temperature of superconducting thin films.) It is also interesting to observe that the increase in global average quality factor change ΔQ at room temperature (from 0.29×10^5 to 0.88×10^5) and decrease in the bi-crystal boundary potential barrier at room temperature (from 33 to 14 mV) are on the same order of magnitude as the transport current improvement.

The interpretation is not straightforward, and is complicated by variations of surface topography and film thickness. The peaks in figures 7 and 8 away from the bi-crystal grain boundary may be associated in part with the morphology of our samples (figures 3 and 4), because both electron microprobe and evanescent microwave measurements are expected to penetrate the full thickness of these samples (0.12 μm for sample A and 0.16 μm for sample B). The large peaks outside but adjacent to the bi-crystal grain boundary for the sample A might be related in part to its higher roughness in the vicinity of the boundary (22.4 nm versus 13.6 nm).

This roughness may not, however, be completely responsible for the distinct bright band of the potential barrier at the bi-crystal grain boundary which is more than twice the size (33 mV versus 14 mV) in sample A than in sample B (see table 1 and figure 10). These results may indicate charge redistribution due to the energy bands bending down and a net charge transfer on the macroscopic scale in the vicinity of the bi-crystal junction causing the junction to carry a positive charge. This has been suggested theoretically in a recent publication [6] and is indicated by our measurements (figures 9 and 10). On the other hand, Kalinin *et al* [12] have shown theoretically that the presence of local charges at the grain boundary of a vicinal and donor-doped $\Sigma 5$ $SrTiO_3$ bi-crystal results in a depletion zone ~200 nm wide, with the interface potential at the middle of the boundary equal to 30 mV. These predictions are not quantitatively consistent with our experimental value of ~1 μm for the width of the region of increased surface potential (figures 5 and 10), however, and other factors may be partially responsible, including substrate, calcium and film thickness effects.

The detailed mechanism for the significantly higher critical current density in sample B requires further investigation, and in particular the effect of substrate temperature should be examined over a wider range. It is, however, clear that high critical current density performance can be achieved with calcium doping without a significant depression of critical temperature, and that evanescent microwave microscopy is a useful probe of doping and conductivity effects. There are indications that room temperature measurements of the change in quality factor and the surface potential in the vicinity of the boundary junction may be correlated with overall critical current density for coated conductor samples, and this requires further investigation.

References

[1] Dimos D, Chaudhari P, Mannhart J and LeGoues F K 1988 *Phys. Rev. Lett.* **61** 219
[2] Hammerl G, Schmehl A, Schultz R R, Goetz B, Bielefeldt H, Schneider C W, Hilgenkamp H and Mannhart J 2000 *Nature* **407** 162
[3] Feldmann D M *et al* 2000 *Appl. Phys. Lett.* **77** 2906
[4] Guth K, Krebs H U, Freyhardt H C and Jooss C 2001 *Phys. Rev.* B **64** 140508
[5] Samara G A, Hammetter W F and Venturini E L 1990 *Phys. Rev.* B **41** 8974
[6] Klie R F, Buban J P, Varela M, Franceschetti A, Jooss C, Zhu Y, Browning N D, Pantelides S T and Pennycook S J 2005 *Nature* **435** 475
[7] Schwingenschlögl U and Schuster C 2007 *Appl. Phys. Lett.* **90** 192502
[8] Schmehl A, Goetz B, Schultz R R, Schneider C W, Bielefeldt H, Hilgenkamp H and Mannhart J 1999 *Europhys. Lett.* **47** 110
[9] Mohan A, Singh K, Kaur N, Bhattacharya S, Dixit M, Gaur N K, Schelke V, Gupta S K and Singh R K 2007 *Solid State Commun.* **141** 605
[10] Su H B and Welch D O 2005 *Supercond. Sci. Technol.* **18** 24
[11] Schofield M A, Beleggia M, Zhu Y M, Guth K and Jooss C 2004 *Phys. Rev. Lett.* **92** 195502
[12] Kalinin S V and Bonnell D A 2000 *Phys. Rev.* B **62** 10419
[13] Haugan T, Barnes P N, Wheeler R, Meisenkothen F and Sumption M 2004 *Nature* **430** 867
[14] Haugan T, Barnes P N, Brunke L, Maartense I and Murphy J 2003 *Physica* C **297** 47
[15] Wang H, Texas A and Univ M 2007 private communication
[16] Kleismit R A, Kozlowski G, Biggers R R, Maartense I, Kazimierczuk M K and Mast D B 2005 *IEEE Trans. Appl. Supercond.* **15** 2915
[17] Kleismit R A, ElAshry M, Kozlowski G, Amer M S, Kazimierczuk M K and Biggers R R 2005 *Supercond. Sci. Technol.* **18** 1197
[18] Viswanathan R and Heaney M B 1995 *Phys. Rev. Lett.* **75** 4433